Cell Reports
Physical Science

CellPress

Article

Metal-Supported Solid Oxide Fuel Cells with Exceptionally High Power Density for Range Extender Systems

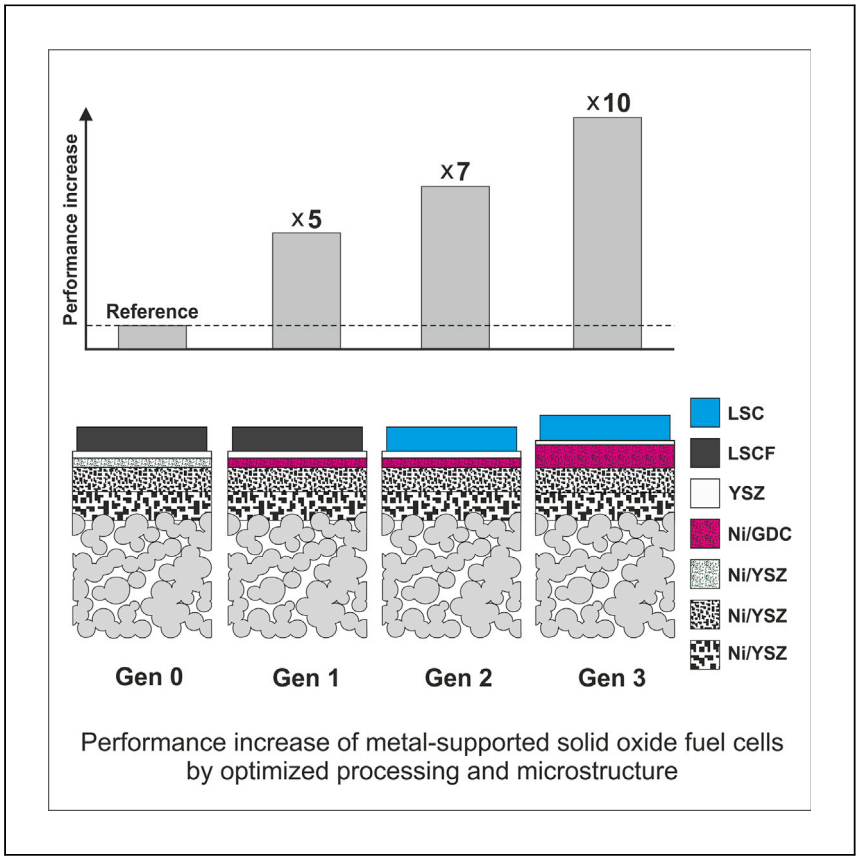

Udomsilp et al. develop a metal-supported fuel cell concept, with potential for application in range extender systems of battery electric vehicles. The authors demonstrate that knowledge-based optimization of this specific cell concept boosts the power density toward the needs of the automotive industry.

David Udomsilp, Jürgen Rechberger, Raphael Neubauer, ..., Alexander K. Opitz, Olivier Guillon, Martin Bram

d.udomsilp@fz-juelich.de (D.U.)
alexander.opitz@tuwien.ac.at (A.K.O.)
m.bram@fz-juelich.de (M.B.)

HIGHLIGHTS

Metal-supported SOFC with current density up to 2.8 A × cm^{-2} at 650°C and 0.7 V

Cell concept is promising for range extender systems in battery electric vehicles

Udomsilp et al., Cell Reports Physical Science *1*, 100072
June 24, 2020
https://doi.org/10.1016/j.xcrp.2020.100072

Cell Reports
Physical Science

CellPress
OPEN ACCESS

Article

Metal-Supported Solid Oxide Fuel Cells with Exceptionally High Power Density for Range Extender Systems

David Udomsilp,[1,3,*] Jürgen Rechberger,[1,4] Raphael Neubauer,[1,4] Cornelia Bischof,[1,3,5] Florian Thaler,[1,3] Wolfgang Schafbauer,[1,5] Norbert H. Menzler,[3] Lambertus G.J. de Haart,[3] Andreas Nenning,[2,6] Alexander K. Opitz,[2,6,*] Olivier Guillon,[3,7] and Martin Bram[1,3,8,*]

SUMMARY

Solid oxide fuel cells (SOFCs) exhibit potential to become a key technology for future clean energy systems. The metal-supported SOFC exhibits decisive strengths like fast start-up capability, mechanical robustness, and acceptable cost, making it the concept of choice for mobile applications. As a promising example, SOFC-powered range extenders for electric vehicles offer fast refueling and significantly increased driving range, while lowering size, weight, and the cost of the vehicle's battery. Here, we report the development of a metal-supported SOFC aiming at exceptionally high power density. A knowledge-based improvement of all electrochemically active cell components enables a performance increase up to a factor of 10 and demonstrates the effectiveness of target-oriented optimization of processing and microstructure. Ultimately, enhanced cells meet the industrial performance target by providing a current density of 2.8 A × cm^{-2} at 650°C and 0.7 V, setting a benchmark for SOFC performance.

INTRODUCTION

Clean electricity generation based on renewables is of vital importance for realizing the international goals set with regard to CO_2 emissions and air pollution in order to limit the global temperature increase caused by greenhouse gases. As reported recently by the International Energy Agency IEA (https://www.iea.org), the mobility sector is a substantial contributor to these emissions, with 24% of the energy-related CO_2 emissions worldwide in 2016. Therefore, significant impact can be achieved by developing alternative powertrains.[1] Whereas the high efficiency of batteries promotes their application, charging time, size, weight, and cost of batteries remain issues still limiting their widespread application.[2,3] Furthermore, large-scale electrification of the individual transport sector based on battery vehicles may be a substantial challenge for power grids, because they need to be capable of satisfying the immense demand of electricity, especially in large urban areas.[3]

A promising concept to overcome these restrictions is the application of a range extender system continuously recharging a small-sized battery.[2,4,5] The fuel cell technology, in general, and solid oxide fuel cells (SOFCs), in particular, are exceptionally well-suited to power automotive range extenders due to their superior efficiency compared to combustion engines, silent operation, and fast refueling. Moreover, systems powered by SOFCs, which work at temperatures of 500°C–800°C,

[1]Christian Doppler Laboratory for Interfaces in Metal-Supported Electrochemical Energy Converters, 52425 Jülich, Germany

[2]Christian Doppler Laboratory for Interfaces in Metal-Supported Electrochemical Energy Converters, 1060 Vienna, Austria

[3]Forschungszentrum Jülich GmbH, Institute of Energy and Climate Research, 52425 Jülich, Germany

[4]AVL List GmbH, Hans-List-Platz 1, 8020 Graz, Austria

[5]Plansee SE, 6600 Reutte, Austria

[6]TU Wien, Institute of Chemical Technologies and Analytics, Getreidemarkt 9/164-EC, 1060 Vienna, Austria

[7]Jülich Aachen Research Alliance, JARA-ENERGY, 52425 Jülich, Germany

[8]Lead Contact

*Correspondence: d.udomsilp@fz-juelich.de (D.U.), alexander.opitz@tuwien.ac.at (A.K.O.), m.bram@fz-juelich.de (M.B.)

https://doi.org/10.1016/j.xcrp.2020.100072

feature remarkable fuel flexibility. This flexibility allows for operation on almost every kind of reformed fuels, because high CO levels can be tolerated.[6,7] Thereby, the SOFC technology breaks free from the restrictions of lacking hydrogen infrastructure, making it both an excellent candidate for the intermediate stage of using existing infrastructure as well as for the operation on biofuels or synthetic CH_4 and also green hydrogen produced from renewables in the future.[2,4,8–10] Consequently, SOFC-based range extenders combine the attractiveness of battery electric vehicles with the convenience of liquid fuels. The high efficiency of electrochemical energy conversion directly corresponds to lower CO_2 emission and enables a virtually particulate-free exhaust gas.

For a near-future realization of range-extender-based electric vehicles, quite stringent boundary conditions such as quick start-up, large fuel flexibility, long service life, high efficiency, and high power output have to be met to economically compete with currently available power train systems. AVL List GmbH defined the following target performance values that have to be met for SOFC-based range extender systems to, on the one hand, be economically competitive with existing systems and, on the other hand, to be technologically realizable yielding a market-ready system within the next years[2,4,5]:

Operation at T <700°C on (1) liquid hydrocarbon fuels for quick refueling based on existing fuel distribution infrastructure, and (2) green H_2 in the future
Quick start-up of the range extender in <15 min
Lifetime: >10,000 h of operation, resulting in service intervals accepted by customers
System efficiency: >50%
Power output: ≥15 kW as a prerequisite for long-distance over-land driving
Current density: single-cell >2.0 A × cm^{-2}
Current density: stack >0.8 A × cm^{-2}
Volumetric power density: stack 1,000–1,200 W × L^{-1}
Volumetric power density: system 100–120 W × L^{-1}
Gravimetric power density: system 120–140 W × kg^{-1}
Degradation rate: <6 mV × kh^{-1}
Cost stack: <100 € × kW^{-1}
Cost system: <200 € × kW^{-1}.

These boundary conditions are in accordance with the targets of the US Department of Energy (DOE) Fuel Cells Technologies Office Multi-Year Research, Development, and Demonstration Plan (FCTO-MYRD&D).[11] This plan defines technical targets for SOFC based auxiliary power units (APUs). DOE targets are dealing more with application of SOFC APUs in heavy trucks, trains, aircraft, or ships and were e.g., used by company Delphi to evaluate their progress of doing pioneering work in the field of APUs for heavy truck applications.[12] Nevertheless, application of APUs as range extender for battery electric vehicles was already mentioned in the early works of Botti et al.[12,13] Because, in the heavy-duty and transportation sector the available space is less restricted than in battery electric vehicles, targets of AVL List GmbH are even more ambitious than DOE targets with respect to power density, system efficiency, and costs.

From the currently known fuel cell types, the metal-supported SOFC has the highest potential to fulfil all these conditions.[9] High thermal conductivity and mechanical stability of ductile porous metal supports are the key to resist quick start-up cycles. Moreover, metal supports provide high robustness against vibrations and redox

cycles, enable reduction of material costs, and ease joining (e.g., by welding).[9,14,15] However, this type of fuel cell is the newest addition to the family of solid oxide cells and thus still suffers from a couple of "teething problems" that need to be solved before metal-supported SOFCs are ready for an application in the mobile sector. In particular, volumetric as well as gravimetric power density, along with prolonged lifetime, remain the major challenges on the way to commercialization of metal-supported SOFCs in the automotive industry.[2,4,16]

To overcome these challenges within a reasonable time frame, a target-oriented development of metal-supported SOFCs is required. Here, we report on a research concept, which is based on a strong synergy of theoretical electrochemical simulations, basic electrochemical studies of individual cell components, and advanced expertise in materials science and processing. Results from fundamental electrochemical studies were introduced in three steps in the cell concept of Plansee SE.[17] Some details of each optimization step have been already published before.[18–21] By combining all measures for the first time in one cell (here called generation three [Gen 3]), we demonstrate an impressive power density of up to 3.13 W × cm^{-2} at 800°C and 0.7 V, approaching an enhancement by a factor 10 compared to the literature.[17,19] Importantly, with a current density of 2.8 A × cm^{-2} at 650°C, Gen 3 cells also meet the performance target of our industrial partner stated above. Preliminary tests hint on long-term stability of single-cells, which are operated under laboratory conditions for up to 1,000 h. All cells used in this study are manufactured on industrial pilot scale with a cell size around 140 × 100 mm^2 from which smaller cells are laser-cut for basic electrochemical investigations. Our results reveal that metal-supported SOFCs with exceptionally high performance can truly be realized, making them utilizable for application in range extender systems, as e.g., developed by AVL List GmbH.[2,4] This development is achieved via a knowledge-based optimization of cell components enabled by the close collaboration of basic science and advanced engineering. The importance of our results is emphasized by benchmarking with other cell concepts. In this context, it is important to highlight that this remarkable increase in power density is achieved by systematic improvement of microstructure and processing, without the need to introduce novel SOFC materials. Such progress is rarely reported in SOFC literature but may be of significant interest to decision-makers, manufacturers, and end-users of SOFC technology, since it shows the potential of the used materials and the technology in general. Finally, the discussion of our results reveals that SOFC-based range extenders have potential to be a key technology for the electrification of our transport and mobility sectors. Furthermore, each optimization step has the potential to be implemented in other SOFC concepts, which may thus lead to improved performance of other SOFC applications.

RESULTS

Fundamental Approach to Boost Electrochemical Performance of Ni/GDC Anodes

A knowledge-based improvement of the cell components, in general, and of the fuel electrode (i.e., the SOFC-anode), in particular, was performed to exploit the full potential of metal-supported SOFCs. Because the metal substrate requires reducing sintering conditions, the processing of the fuel electrode is considerably different from established SOFC concepts and therefore needs individual development. This development was guided by a basic understanding of the employed materials and their interaction in the fuel electrode. Supported by experiments on model systems,[22] as well as by electrochemical simulations,[23] the polarization resistance of the anode was broken down to the level of physical elementary parameters. Linking

experimental data, results of simulations, and materialographical investigations of the electrode, allowed identifying the most efficient approaches for minimization of the anode polarization resistance and thus was the key for maximizing the cell performance.

Unlike the pure ion conductor Yttrium-doped zirconia (YSZ) in common SOFC anodes, Gadolinium-doped ceria (GDC) is a mixed ionic electronic conductor (MIEC) under the reducing conditions at the fuel electrode.[24,25] Owing to its mixed valence of Ce^{3+}/Ce^{4+}, it also acts as an excellent catalyst for the anodic fuel oxidation reaction, which proceeds on the entire GDC surface.[26] From this in-depth understanding of GDC's elementary properties and their role for the electrochemical reaction in the Ni/GDC cermet, we can deduce that the Ni phase is mainly necessary for the long-range electron transport and mechanical stability, whereas fine GDC particles distributed over the Ni scaffold promote electro-catalytic activity as well as ion transport and local electron collection. This job-sharing situation is sketched in Figure 1A and can be modeled by a transmission-line-type equivalent circuit[23,27–30] that also considers the chemical capacitance of the GDC phase.[31,32] For fitting of impedance data (see below), elements considering (minor) resistive and capacitive effects of the electrode/electrolyte interface and the ohmic resistance of the electrolyte must be added; the resulting circuit is depicted in Figure 1B. From this circuit and the position of the resistors of the electrochemical reaction on the GDC surface and ion conduction in its bulk, it can be deduced that a high surface area and a low tortuosity of the GDC phase are crucial for a low anode polarization resistance.

Therefore, the optimized microstructure of our Ni/GDC anode is rather unconventional (see Figure 2)—the Ni phase is much coarser than the GDC phase and the anode thickness needs to be relatively large. This anode thus breaks two yet believed essential rules of SOFC anode processing: finely dispersed microstructure of both phases and limited thickness to avoid gas transport limitations. However, even if—in comparison to established SOFC anodes—sub-optimal at first glance, such structure perfectly exploits the potential of the used materials and the electrochemical reaction pathways in the cermet. As a consequence, the polarization resistance of our Ni/GDC fuel electrodes is relatively small as can be seen in Figure 1C.

In this image, a typical impedance spectrum measured on a symmetrical cell at 750°C (symbols) is plotted together with the obtained fit curve (lines) using the circuit from Figure 1B. From the corresponding fit results and the geometry parameters of the electrode, the ionic conductivity and the surface reaction resistance of GDC can be calculated (see Supplemental Experimental Procedures with Figures S1 and S2 for details and more impedance data). At 750°C, we get an ionic conductivity $\sigma_{ion} = 0.06\ S \times cm^{-1}$ and a GDC surface-area-specific resistance $R_{react} = 2\ \Omega \times cm^2$, which are in excellent agreement with literature values of $0.06\ S \times cm^{-1}$ [33] and $4\ \Omega \times cm^2$,[34] respectively, thus proving the physical validity of the model. Thanks to the excellent agreement of impedance fitting results to electrode thickness variation we can verify that the GDC phase tortuosity is rather low (~3), compared to values published for Ni-YSZ cermets.[35–37] Due to the very different Ni and GDC particle sizes, most GDC particles are ionically connected, which is most likely the origin of this low tortuosity of the GDC phase. Together with the high GDC surface area, this low tortuosity is jointly responsible for the low anode polarization resistance and thus the high cell performance.

The respective microstructure of an optimized metal-supported SOFC shown in Figure 2 confirms small and homogeneously distributed GDC particles on a coarse Ni

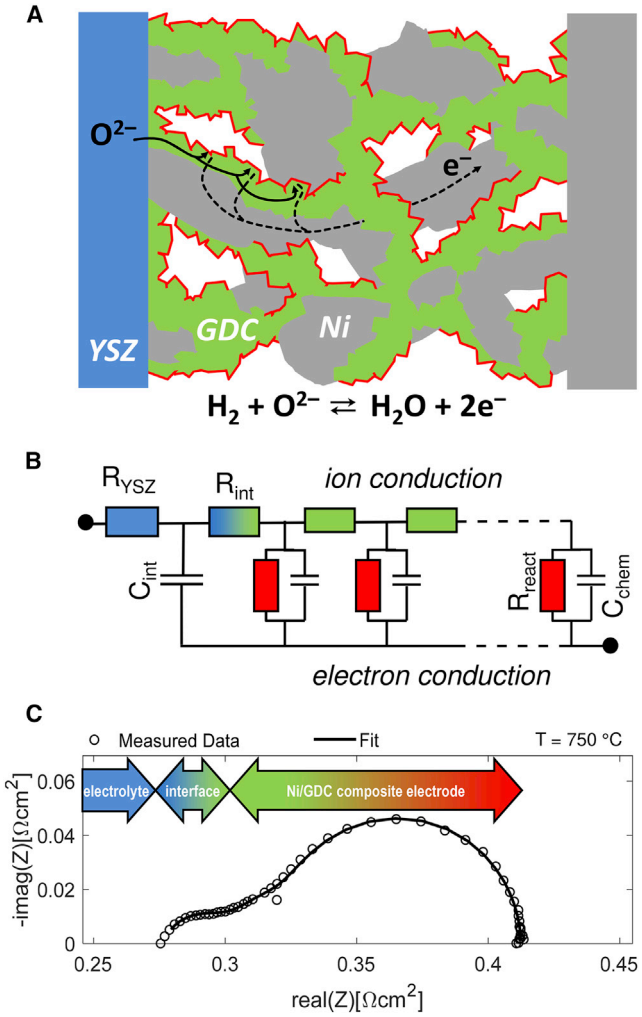

Figure 1. Predicting Optimum Microstructure of Ni/GDC Cermets by a Fundamental Electrochemical Approach

Electrochemical performance of the fuel electrode.

(A) Sketch of the current pathways in the Ni/GDC cermet for oxide ions (solid arrows) and electrons (dashed arrows). The electrochemical fuel oxidation reaction proceeds on the free GDC surface, which is highlighted by the red color.

(B) Equivalent circuit representing the electrochemical current pathways and the physical elementary parameters of the involved materials. For a percolating Ni phase, the resistances of the electronic rail are very small (σ_{eon} of Ni is ca. 10^5 S x cm^{-1}); for fitting purposes, this rail was thus short-circuited.

(C) Typical impedance spectrum (Nyquist plot) measured on a symmetrical model cell with 6-μm thick Ni/GDC cermet anode (circles) together with fit curve (line) employing the circuit in (B). To demonstrate the reproducibility of the anode impedance and to show the effect of different functional layer thickness, additional impedance results are shown in Figures S1 and S2.

network. In addition to high catalytic activity for fuel oxidation, this novel kind of anode microstructure has even further advantages like (1) sufficient mechanical stability and suitably low surface roughness for subsequent electrolyte coating via so-called gas flow sputtering,[18] (2) low risk of Ni coarsening and related degradation phenomena even at operating temperatures up to 800°C, and (3) enhanced redox stability compared to established Ni/YSZ anodes as demonstrated recently.[15] Furthermore, it is expected that this microstructure might be even attractive for

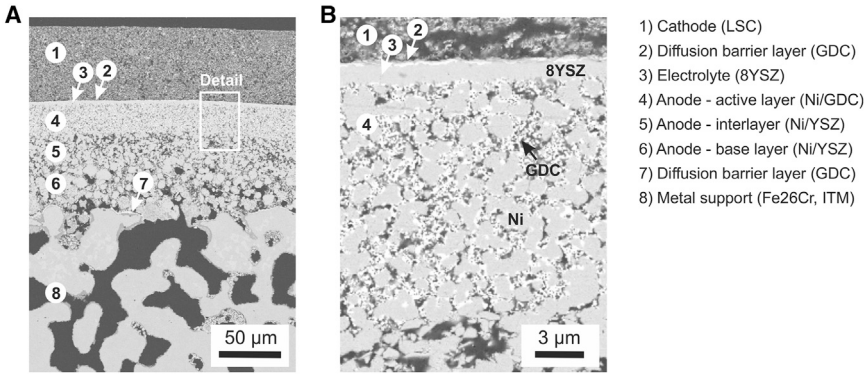

Figure 2. Implementation of Ni/GDC Cermet Electrode with Optimized Microstructure in Gen 3 Cells

(A and B) Microstructure of a Gen 3 metal-supported SOFC (A) cross-section showing all layers of the cell, (B) optimized Ni/GDC anode design with coarse Ni network and finely dispersed, electrochemically active GDC phase (large gray particles, Ni; small white particles, GDC).

operation in electrolysis mode, but related investigations are still pending and part of our future work. In order to arrive at sound conclusions on its suitability, investigation of electrolysis-specific degradation phenomena (e.g., reported in literature for solid oxide cells with Ni/YSZ electrode[38,39]) will be an important part of this future work.

Stepwise Increase of Cell Performance by Improving Electrodes and Electrolytes

Starting from the reference cell (Gen 0) representing the state-of-the-art metal-supported SOFC from Plansee SE with Ni/YSZ anode,[17,40,41] the cell was improved stepwise as described in more detail in the Experimental Procedures. In Gen 1, the Ni/YSZ anode was replaced by Ni/GDC with optimized microstructure according to our fundamental study described before.[19] The electrochemical performance of the Gen 1 cell confirms the enhanced catalytic activity of the cermet thus proving our approach. Gen 2 features a cell with highly active LSC cathode, therefore increasing catalytic activity also on the air side.[20,21] Finally, Gen 3 cell combines for the first time these highly active electrode materials with the thin-film electrolyte and the increased thickness of the active anode layer derived from the basic science section. The electrochemical performance of the Gen 3 cell at operating temperatures between 650°C and 800°C is demonstrated in Figure 3 by current versus voltage curves (I-V-curves). Due to the outstanding performance of the cell, the maximum current load of the available test rig is exceeded for 0.7 V at each temperature. Therefore, current densities at 0.9 V were chosen for a direct comparison of measured performance values. Additionally, the I-V-curves were extrapolated to a cell voltage of 0.7 V, which is a more common operating point for performance benchmarks. Because the I-V-characteristics show an almost linear behavior between ca. 1.5 and 2.0 A × cm^{-2}, this extrapolation can be done with acceptable accuracy and helps to benchmark the cell performance to published literature. Related extrapolations have already been used before in literature for evaluating SOFC performance.[42] The apparent hysteresis between the values measured with increasing and decreasing current is due to Joule heating of the cell. To avoid overestimation of the cell performance, the lower values are displayed in the following plots. For details, please see the section "Electrochemical Testing of Metal-Supported Fuel Cells" in the experimental part. At the highest temperature of 800°C, current densities of 1.77 A × cm^{-2} and 4.47 A × cm^{-2} were measured/extrapolated at 0.9 V

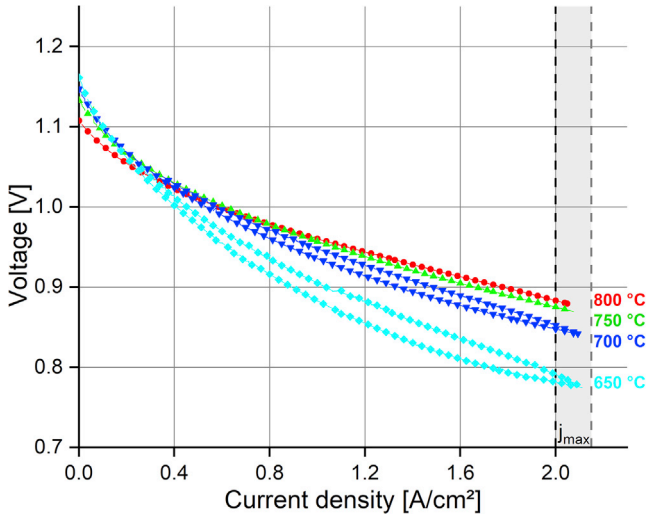

Figure 3. Electrochemical Performance of Gen 3 Cells

I-V-characteristics of the Gen 3 metal-supported SOFC at operating temperatures between 650°C and 800°C. 50 × 50 mm^2 cell with 16 cm^2 active cathode area. Gas supply, 1,000 sccm H_2, 2,000 sccm air.

and 0.7 V, respectively. This corresponds to power densities of 1.59 W × cm^{-2} and 3.13 W × cm^{-2}, which is among the highest ever published values for SOFCs in general and the highest for metal-supported SOFCs in particular.

Figures 4A and 4B illustrate the development of cell performance from Gen 0 to Gen 3 for 0.7 V and 0.9 V, respectively. Ultimately, the development of Gen 3 led to an enhancement of the single-cell power density by up to a factor of 10 compared to Gen 0, as also shown in Figures 4A and 4B. The achieved performance of the highest performing cell type (Gen 3) is compared with results from literature for other metal- as well as anode-supported cells in Figures 4C (0.7 V) and 4D (0.9 V), revealing a superior performance level of our Gen 3 cells. For a more detailed performance benchmarking with other metal-supported SOFC concepts reported in the literature, the reader is referred to the Note S1 and Table S1.

It is particularly worth emphasizing that the Gen 3 metal-supported cell also outperforms the most advanced anode-supported SOFC (ASC) from Jülich featuring a 1-µm thin electrolyte,[42,43] which already served as a major reference value for several SOFC benchmarks. This higher performance despite the larger thickness of the electrolyte confirms the effectiveness of the implemented measures in cell optimization from Gen 0–Gen 3. Especially the performance boost realized by moving from Gen 2 to Gen 3 emphasizes that microstructure and processing optimization can have an equally important impact on cell performance as introduction of novel electrode materials. Furthermore, by avoiding introduction of completely novel and thus insufficiently characterized materials, the risk of unexpected side effects like unknown, material-specific degradation phenomena is reduced, which is an important aspect for a successful transfer of the technology to industry.

Preliminary Testing of Long-Term Stability

Besides the efforts to achieve high-performance cells, preliminary long-term stability tests with humidified fuel gas were conducted using Gen 2 cells. Overall test durations covered up to 1,000 h with more than 400 h of operation under a 50/50 H_2/

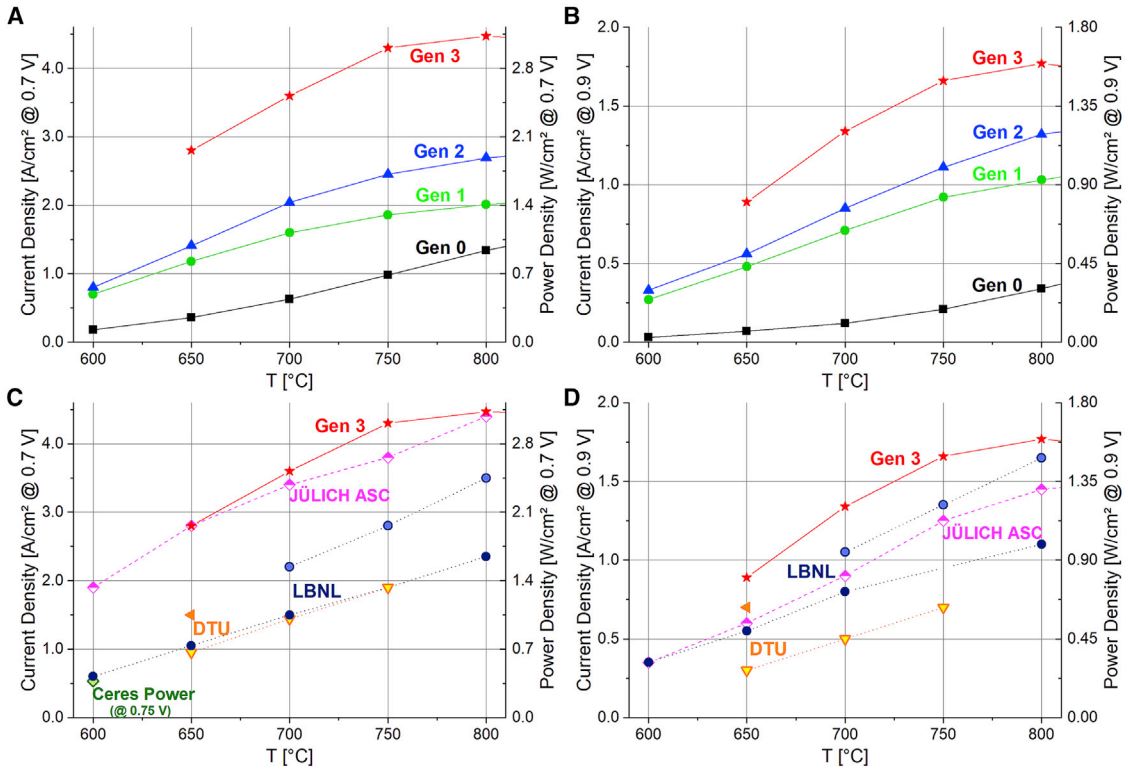

Figure 4. Evolution of Electrochemical Performance from Gen 0 to Gen 3 Cells and Benchmark to Other Cell Concepts

(A and B) Increase of current and power density by systematic processing and microstructure optimization of the metal-supported SOFC in 3 cell generations at cell voltages of (A) 0.7 V and (B) 0.9 V.

(C and D) Performance benchmark by comparison of Gen 3 with literature data of the JÜLICH ASC[42,43] and metal-supported SOFCs from LBNL,[45,46] DTU,[47,56] and Ceres Power[48] at cell voltages of (C) 0.7 V and (D) 0.9 V. For a more detailed benchmark of published MSC results see Table S1.

H_2O mixture as fuel gas. Figure 5A shows the long-term behavior at a current density of 300 mA × cm^{-2}. First, 230 h of the test were conducted with dry fuel gas, then the fuel gas was switched to humidified conditions. Another 292 h of operation were achieved with current load under humidified conditions (total humidified period: 432 h). Unfortunately, during this cell test, current and humidification were partly interrupted due to malfunction of the experimental setup, which leads to the somewhat uncommon appearance of the test results in Figure 5A. A degradation rate of <5 mV per 1,000 h was observed indicating that the cell performance was not significantly changed under the given testing conditions. This result was confirmed by I-V measurements in dry and humidified fuel gas before and after continuous operation.

Post-mortem analysis of the Gen 2 cell by SEM after the long-term test revealed a slightly oxidized metal support at the pore walls and at the interface to the GDC diffusion barrier layer. Furthermore, we observed beginning oxidation of Ni grains adjacent to the diffusion barrier layer (Figures 5B and 5C).[44] Energy-dispersive X-ray spectroscopy (EDX) analysis revealed the formation of a Cr_2O_3 scale at positions marked with an arrow. Figure 5C hints on increased oxidation of sintering necks, but further investigations are required to conclude on this. In the coarse porous anode layer adjacent to the metal substrate (base layer in Figure 2), diffusion of Fe and Cr into the Ni particles was found, which we suggested being the reason of oxide scale formation on the Ni particles (Figure 5B). In contrast, Fe and Cr

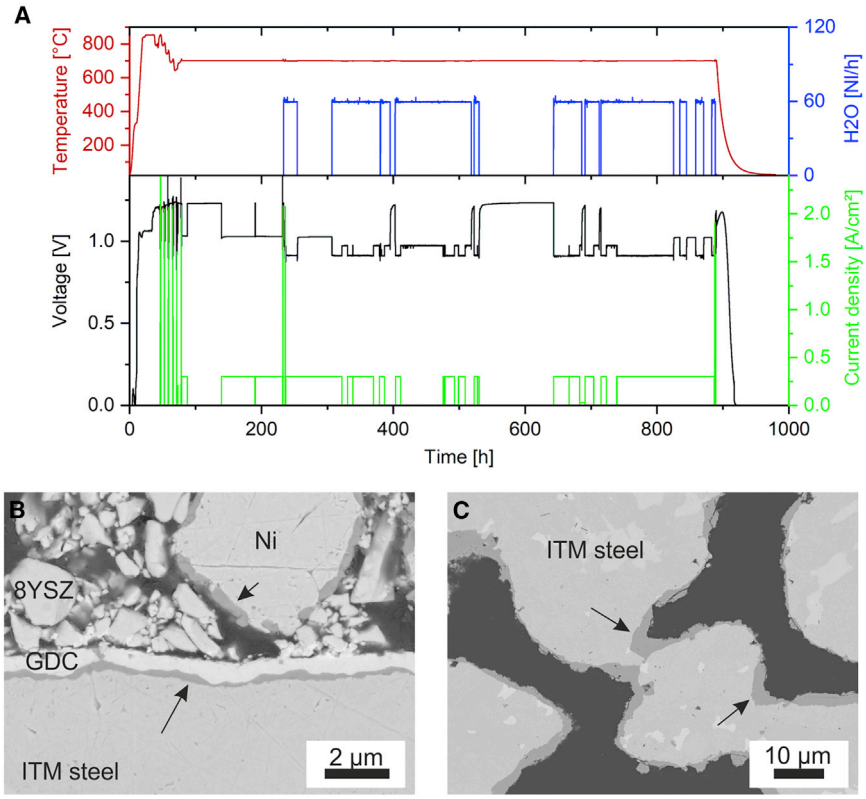

Figure 5. Preliminary Long-Term Test of Gen 2 Cells with Humidified Fuel Gas

(A) Cell voltage of a Gen 2 cell (Ni/GDC anode functional layer, LSC cathode) during a two-step degradation test at 700°C and constant current load of 300 mA cm^2 over 900 h. First period: dry H_2 fuel. Second period: 50% humidified H_2.

(B and C) Post-mortem analysis after cell test showed (B) formation of Cr_2O_3 scales at the interface to the diffusion barrier layer and adjacent Ni grains and (C) increased formation of Cr_2O_3 scales at sintering necks. Cr_2O_3 scales were analyzed by EDX and are marked by arrows. Adapted from Thaler et al.[44]

concentration in the active Ni/GDC anode layer was below the detection limit and therefore, we did not observe oxidation of Ni phase in the electrochemically active zone. To clarify when interdiffusion mainly takes place, EDX investigations on as-prepared cells were performed as a reference. These measurements revealed that Fe and Cr diffusion already occurred during sintering of the anode layers mainly due to the higher temperature. The diffusion barrier layer reduced but not completely prevented Fe and Cr diffusion. This observation might be caused by geometrical restrictions at positions where the anode layer penetrates the outer pores of the metal substrate. Caused by the specific coating mechanism of PVD, only the surface of the metal substrate is coated by the diffusion barrier layer.

These preliminary results of operating the cell for 1,000 h at 700°C under humid fuel conditions suggest that the specific cell design of the metal-supported SOFC has the potential for application in real range extender conditions. Because between the Gen 2 and Gen 3 cells only the thickness of both the electrolyte and the anode layer were changed, but the materials and processing parameters were kept the same, it is expected that the degradation results of Gen 2 cells can be also regarded as representative for Gen 3. Unfortunately, a related measurement failed due to malfunction of the testing device. In conclusion, we must acknowledge that the results in the

present state are preliminary and further systematic long-term tests are required—both in lab conditions as well as in real range extender systems applying a suitable stack design—to draw sound conclusions on the future applicability of this cell concept.

DISCUSSION

Application of metal-supported SOFC technology in range extenders of battery electric vehicles is quite challenging due to limitations in available space. System performance in the range of 20–30 kW combined with a volumetric power density (stack level) of 1,000–1,200 W × l^{-1} at operation temperatures below 700°C—as aspired by AVL List GmbH on a midterm scale[4]—can only be realized if the current density of the cells exceeds 2 A × cm^{-2} (see Introduction). At the beginning of our target-oriented development of the Plansee SE cell concept in 2016, all published performance values of metal-supported SOFCs were far below this value. For more details, see Table S1. Our research hypothesis was to optimize the electrochemically active layers almost independently of each other enabling better understanding of the relationship between processing, microstructure, and resulting electrochemical performance for each layer.[18–21] As exemplarily described for the anode in the first part of the Results, in all cases, fundamental electrochemical studies on model electrodes were the starting point of development.[22,23,29,30,34] Furthermore, we decided to focus our research on established SOFC materials to avoid unforeseeable degradation phenomena and interface reactions. The improvements achieved by this approach were implemented step by step in the pilot manufacturing at Plansee SE resulting in Gen 1 and Gen 2 cells, which already show current densities near to the target value. In the present work, all efforts were combined for the first time in Gen 3 cells, which are characterized by a Ni/GDC anode, where the thickness was adapted, a 2-μm thin electrolyte and a high performing LSC cathode. As main result of our study, the performance of Gen 3 cells is among the highest ever published values for SOFCs in general and the highest for metal-supported SOFCs in particular (Figures 4C and 4D). It is expected that system requirements regarding volumetric and gravimetric density can be fulfilled if such current densities can be at least partly transferred to stack level. Our results are—in our opinion—of high interest for other research groups working on SOFC technology, because they demonstrate how target-oriented optimization of processing and microstructure of SOFC electrodes can be used to boost electrochemical performance. The advantage of Ni/GDC anodes and their specific processing resulting in a—compared to full ceramic fuel cells—unconventional microstructure with a coarse and stable Ni network covered by small interconnected GDC particles might be of special interest for other SOFC concepts as well. This microstructure is expected to be quite stable against Ni coarsening and redox cycling. The latter has been proven recently.[15] In the last few years—driven by the automotive industry—significant performance increase was also reported for the cell concepts of Lawrence Berkeley National Laboratory (LBNL)[45,46] and Technical University of Denmark (DTU).[47] For both cell concepts, infiltration technologies were applied to achieve high performing, nanostructured electrodes. It is suggested by the authors that during long-term operation, these nanostructures are sensitive to coarsening, which might become the reason for proceeding cell degradation. Another metal-supported SOFC concept is pursued by Ceres Power (UK) focusing on low-cost cell fabrication, rather than maximizing performance.[48] Accordingly, operating conditions and cell requirements differ from other cell concepts. Strategic collaborations in industrial-scale stack manufacturing were established with Weichai Power (China) for range extender development and Robert Bosch GmbH (Germany) for stationary power supply and application in

data centers.[49] For more details on running cooperation of Ceres Power, we refer to https://www.ceres.tech/. Recently, General Electric even demonstrated the potential of metal-supported SOFCs for stationary power supply in the several 10 kW range.[50] To achieve stringent cost reduction, they used thermal spray technologies in combination with punched and brazed sheet-metals to overcome traditional stack design constraints. Concerning these multiple industrial activities, it becomes obvious that the relevance of metal-supported technology is not necessarily a matter of mobile applicability, but also considered for stationary systems depending on purpose and boundary conditions. In general, we believe that all results of advanced metal-supported SOFCs are significant for the industrial end-users and decision-makers since they demonstrate the huge potential of the metal-supported SOFC technology for a variety of applications. Furthermore, we believe that some of our results can be easily integrated into other cell concepts like the application of an optimized Ni/GDC anode in the concept of General Electric.

A novel application of metal-supported SOFCs is the reversible operation in fuel cell and electrolysis mode. Recently, the first related results were published by Wang et al.[51] If operating established full ceramic SOFCs in electrolysis mode, it was reported by several authors that cermet anodes, which are proven for their long-term stability under SOFC conditions, show a specific new degradation phenomenon if operated in electrolysis mode.[52–54] After operation for several 1,000 h in electrolysis mode, agglomeration and depletion of Ni from the electrochemically active zone led to much higher cell degradation than in fuel cell mode. Up to now, the underlying mechanism of Ni depletion is still unknown. Investigating the electrochemical performance and specific degradation of our optimized Ni/GDC cermet electrode when operated under electrolysis conditions would be of high interest and will be part of our future work.

Up to now, only preliminary electrochemical degradation studies were conducted for evaluation of the long-term stability of the Plansee SE metal-supported SOFC concept. The studies were done on a Gen 2 cell for up to 1,000 h with humidified fuel gas (H_2/H_2O mixture with 50/50 ratio) at 700°C and a current density of 300 mA × cm^{-2}. Under these relatively mild conditions, no obvious cell degradation was observed. This result can be explained as follows. First, post-mortem analysis of the cell indicated that growth of Cr_2O_3 scale on the metal support took place at a quite moderate rate. Second, even if a GDC diffusion barrier layer is placed between metal support and Ni/YSZ base layer (Figure 2), diffusion of Fe and Cr into the Ni phase could not be completely avoided. If exceeding a critical value, Cr in the Ni phase is expected to trigger formation of an electrochemically inactive Cr_2O_3 scale. SEM/EDX analyses of the cell before and after long-term operation[44] reveals that such interdiffusion mainly took place during processing (sintering of the anode layers under H_2 atmosphere at temperatures in the range of 1100°C–1200°C) and was not aggravated during cell operation. Post-test analysis of the active Ni/GDC anode layer after long-term operation showed very low Cr concentration and no oxidation in this area. Third, our specific anode design with coarse porous Ni network and finely dispersed GDC particles on its surface was found to be resistant against further coarsening of microstructure during operation at 700°C. Based on this observation, we expect an advantage regarding long-term stability compared to cell concepts with infiltrated electrodes, but further long-term studies under more realistic range extender conditions are required to prove this assumption.

Whereas suitability for pilot scale manufacturing was confirmed, implementation of the cell in an adapted stack design and testing of these stacks in range extender

systems were not demonstrated yet. Therefore, an objective and comprehensive assessment of the suitability of the Plansee SE cell concept for long-term operation under range extender conditions needs to be done in future studies.

In summary, range extender systems for battery electric vehicles powered by SOFCs present a very promising technology for the near-future electrification of the mobility sector, because they enable increased driving range in combination with fast refueling and reduced size of the required battery. Metal-supported SOFCs, in particular, are predestined to fit the requirements of electromobility such as quick start-up, cyclic operation, and fuel flexibility. However, high performance is a prerequisite for a successful implementation.

Our results demonstrate that suitably combining the efforts of fundamental science and advanced engineering on pilot scale enables major improvement of the electrochemical performance of metal-supported SOFCs. The successful deconvolution of the fuel electrode impedance by using methods of basic electrochemistry provided the understanding for the design of a novel Ni/GDC anode microstructure, which was one of the main keys for the high performance of the metal-supported SOFCs in this work. In accordance with the theoretical calculations, the implementation of finely structured GDC into the fuel electrode and an optimized thickness of the anode layer proved to be a significant measure to enhance cell performance. For the first time, this optimized anode structure was combined with a 2-μm thin-film electrolyte and a highly active LSC cathode, resulting in a performance increase up to a factor of 10 without the need to introduce novel materials. The obtained Gen 3 metal-supported SOFC outperformed even state-of-the-art anode-supported SOFCs, thus setting a new benchmark for SOFC development and demonstrating how an in-depth understanding of fundamental materials properties and their electrochemical interplay provides the basis for a knowledge-based optimization of SOFCs. In addition, preliminary tests confirmed long-term stability of the Gen 2 cells for up to 1,000 h of operation with negligible degradation.

Consequently, metal-supported SOFCs have the potential to play a key role in the implementation of range extender systems in battery electric vehicles. The presented results reveal that microstructure and processing optimization is a strong measure to boost cell performance and encourage other developers of SOFC technology to strengthen efforts on this topic. As the next steps of development, cost reduction of the fabrication, development of a robust stack design and demonstration of long-term stability in a real range extender system are considered most important.

EXPERIMENTAL PROCEDURES

Resource Availability

M.B. discloses as Lead Contact any restrictions regarding distribution of materials and protocols to other qualified researchers. The authors support the intention of the journal that other researchers can reproduce or build on their own work on the results published in this work.

Lead Contact

Further information and requests for resources should be directed to the Lead Contact, M.B. (m.bram@fz-juelich.de).

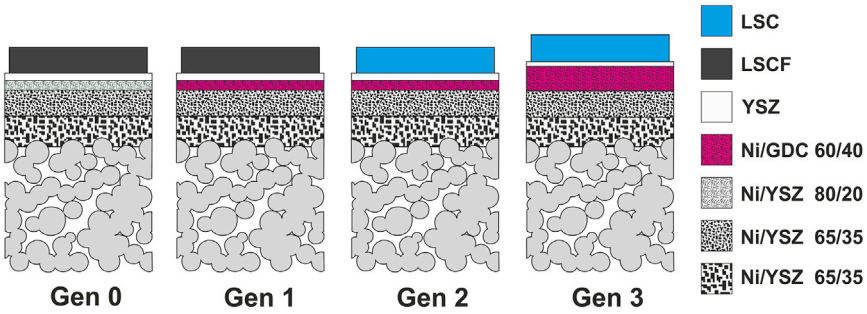

Figure 6. Stepwise Optimization of Processing and Microstructure of the Metal-Supported Solid Oxide Fuel Cell (Plansee SE concept)

Schematic summary of all measures implemented in three cell generations resulting in the demonstrated improvement of cell performance. Ni/ceramic ratio given in wt %

Materials Availability

All metal-supported solid oxide fuel cells investigated in this work were produced on pilot scale at Plansee SE. As starting materials, commercial powders were used. The main outcome of the work was significant improved processing and microstructure of metal supported solid oxide fuel cells. For more details on cell manufacturing and availability of cells manufactured on the pilot plant, we refer to W.S. from Plansee SE, who is co-author of this manuscript. For reproducible cell production, Plansee SE applied quality assurance measurements fulfilling industrial standards. Furthermore, we refer to our related publications cited in the subchapter on manufacturing of metal-supported cells.

Data and Code Availability

The authors declare that data supporting the findings of this study are available within the paper and the Supplemental Experimental Procedures including Figures S1 and S2. All other data are available from A.K.O. and M.B. upon reasonable request.

Manufacturing of Metal-Supported Fuel Cells

All metal-supported SOFCs used in this work were fabricated on a highly porous 300-μm thick ferritic oxide dispersion-strengthened Fe-Cr alloy (Intermediate Temperature Metal ITM from Plansee SE, Austria). The size of the substrates was around 140 × 100 mm^2. For single-cell testing, smaller dimensions of 29 mm Ø or 50 × 50 mm^2 were achieved by laser cutting respective pieces from real full-sized cells. Figure 6 shows the stepwise change of the Plansee SE cell concept aiming at improving electrochemical performance. For a general description of cell fabrication at Plansee SE, we refer to the literature.[17] In the work of Haydn et al.,[17] Gen 0 cells were developed closely mirroring traditional anode-supported cells with Ni/YSZ anode, thin-film 8YSZ electrolyte, and $La_{0.58}Sr_{0.4}Fe_{0.2}Co_{0.8}O_{3-\delta}$ (LSCF) cathode. The Plansee SE cell concept contains a three-layered Ni/YSZ anode with decreasing surface roughness and pore size enabling to coat a gas-tight, 4-μm thick 8YSZ electrolyte via gas flow sputtering. All anode layers were deposited by screen printing starting from mixtures of metallic Ni and 8YSZ powder. It was found that a Ni/YSZ ratio of 80/20 in the top layer was advantageous to achieve high gas tightness of the electrolyte. Sintering of all anode layers was done in reducing H_2 atmosphere at temperatures in the range of 1,100°C–1,200°C to avoid severe oxidation of the metallic substrate.[19] After sputtering of the electrolyte, the LSCF cathode was screen printed and *in situ* activated at 800°C during onset of cell operation. To avoid severe interdiffusion at the interfaces, magnetron sputtered GDC barrier layers were deposited between metal support and Ni/YSZ anode and between electrolyte and cathode.

In Gen 1 cells, Ni/GDC was implemented leading to enhanced catalytic activity of the cermet as predicted from fundamental electrochemical studies.[19,23] Lowering the Ni content to 60 wt % and reduction of sintering temperature to 1100°C was found to be necessary to avoid pronounced Ni coarsening in the presence of GDC. In Gen 2, the *in situ* activated LSCF cathode was replaced by a highly active $La_{0.58}Sr_{0.4}CoO_{3-\delta}$ (LSC) cathode, significantly increasing catalytic activity also on the air side. Comprehensive studies were conducted to replace *in situ* activation by ex situ sintering under protective atmosphere[20] and implementation of LSC/GDC dual-phase cathodes.[21] However, the best electrochemical performance was still achieved by *in situ* sintering of LSC. Finally, Gen 3 combines the highly active LSC cathode material with the Ni/GDC anode and thus compiled all efforts to optimize the Plansee SE cell concept in one cell and testing of its electrochemical performance was done for the first time in the present work. Especially, thickness (22 μm) and microstructure of the active Ni/GDC anode were further improved increasing the electrochemically active volume while in parallel enabling deposition of a 2-μm thin-film electrolyte according to the work of Bischof et al.[18] The increased active layer thickness is a direct consequence of the basic electrochemical investigations (see first part of Results). The region of electrochemical reaction decays from the electrolyte into the porous Ni/GDC anode, and the entire electrochemical reaction takes place within a zone of 3 × λ ($\lambda = \sqrt{(R_{react}\sigma_{eff})}$ (see Supplemental Information). For the optimized Ni/GDC anodes, λ amounts to 5–6 μm (see Figure S2D) and thus 15–18 μm active layer thickness are required for fully exploiting their potential. The applied thickness of 22 μm was therefore chosen to safely meet this requirement. Consequently, the Ni/YSZ 65/35 inter- and base layer do not play any role in the electrochemical reaction. On the one hand, their function is to reduce the pore size and roughness from the substrate to the functional layer, and on the other hand, their function is to collect the electronic current from Ni/GDC.

Electrochemical Characterization of Ni/GDC Fuel Electrodes

For basic characterization of Ni/GDC electrodes, symmetrical electrolyte-supported model cells were fabricated. For details, we refer to the related literature.[19] The symmetrical cells were electrochemically characterized in an atmosphere containing 45 mbar H_2 and 25 mbar H_2O, mimicking 35% of fuel utilization. The reduced total pressure of 70 mbar was chosen to increase the gas diffusion coefficients, thus suppressing resistive contributions from gas phase diffusion. For impedance measurements, the symmetrical cells were electrically contacted by a highly porous Ni foam in a custom-made sample holder (Huber Scientific, https://www.sofc.at). Impedance spectroscopy in a frequency range of typically 10 mHz to 1 MHz was performed at temperatures between ca. 580°C and 810°C using a N4L phase sensitive multimeter 1735 with IAI impedance analyzer (both: Newtons4th Ltd., https://www.newtons4th.com).

Quantitative analysis of impedance spectra was done by complex non-linear least-squares (CNLS) fitting employing the equivalent circuit in Figure 1B (software: Z-View 3.4, Scribner Associates, Inc., https://www.scribner.com). Fit results for the Ni/GDC cermet electrode at all experimental temperatures and a comparison of the respective elementary parameters with literature values are shown and discussed in the Supporting Information.

Electrochemical Testing of Metal-Supported Fuel Cells

The manufactured metal-supported SOFC full-cells with green (i.e., not sintered) cathode are assembled in the test setup between two thin YSZ frames using a glass sealant developed at Forschungszentrum Jülich.[55] The outer dimensions of the

metal support were 50 × 50 mm^2. The size of the active cathode area was 40 × 40 mm^2. During initial heating of the setup, the glass melts and ensures a gas-tight sealing. A dwell time of 10 h at the sealing temperature of 850°C is set for crystallization of the sealant and "in situ activation" of the cathode. This term is chosen to differentiate between common sintering processes during cell manufacturing and thermal treatment within the test setup.

Electrochemical characterization is performed using a commercial test rig from EBZ GmbH (Dresden, Germany). Homogeneous gas supply is ensured by the use of a channel design flow field feeding either dry H_2 or a 50/50 H_2/H_2O mixture to the fuel compartment with a flow rate of 1,000 sccm H_2. Air is fed to the cathode as an oxidant at 2,000 sccm. A Pt mesh is used for the cathode contact and a Ni mesh as current collector at the fuel side. Current-voltage curves are measured from 0–32 A (max 34 A) between 800°C and 650°C in steps of 50 K. The maximum fuel utilization amounts to 22% resulting from the fuel flow rate and the maximum current of the test rig.

IV curves are extrapolated to a theoretical operation point of 0.7 V in order to compare the performance to previous experiments. An extrapolation of the measured data points with a linear slope close to the maximum current load of 2 A × cm^{-2} is used. A possible impact of concentration limitation can be neglected, due to the low fuel utilization of $\leq$22%. Additionally, benchmarking of measured cell performance is performed at a cell voltage of 0.9 V, to exclude the influence of extrapolation errors. Moreover—as can be seen in Figure 5—the high current load leads to an increase of the cell temperature due to Joule heating, which in turn results in an apparent increase of the cell performance visible from the bending of the (otherwise linear) IV curve and a hysteresis-like appearance in the plotted graph between increasing and decreasing current. This is a common issue when testing larger cells but complicates the assessment of extrapolated values.

For a conservative estimate of the presented performance, values for 0.7 V are extrapolated from the data points of decreasing current, whereas the values measured at 0.9 V are derived during increase of the current. This is as the cell temperature tends to further increase while decreasing the current, resulting in a steeper slope and thus in lower current densities extrapolated for 0.7 V. In contrast, the cell temperature is closer to the setpoint during increase of the current load, whereas the progress of the curve while decreasing the current would overestimate the cell performance when relating it to the set temperature.

For estimating the long-term stability of metal-supported SOFCs, electrochemical tests were conducted for up to 1,000 h. In the first 7 days, the cell was operated with dry hydrogen. Gen 2 cells were mounted in the test rig and an initial I-V performance check between 800°C and 650°C was done at the beginning of the test. Then the cell was continuously operated at 700°C with a current density of 300 mA × cm^{-2} for 100 h. Afterward, fuel gas composition was changed to a target value of 50 vol.% humidified H_2. I-V curves were measured at 700°C before and after 100 h operation under dry fuel and at beginning and end of operation with humidified fuel gas, followed by a final performance check using dry fuel.

SUPPLEMENTAL INFORMATION

Supplemental Information can be found online at https://doi.org/10.1016/j.xcrp.2020.100072.

ACKNOWLEDGMENTS

The authors would like to thank T. Brambach and C. Tropartz for conducting the electrochemical tests and Dr. D. Sebold for SEM analysis. Furthermore, the authors gratefully acknowledge funding of the Christian Doppler Laboratory for Interfaces in Metal-Supported Electrochemical Energy Converters by the Austrian Federal Ministry for Digital and Economic Affairs (BMDW) and the National Foundation for Research, Technology, and Development.

AUTHOR CONTRIBUTIONS

Conceptualization, M.B., W.S., J.R., and A.K.O.; Methodology, M.B. and A.K.O.; Investigation, D.U., C.B., F.T., and A.N.; Resources, W.S., N.H.M., L.G.J.d.H., A.K.O., and M.B.; Writing – Original Draft, D.U., A.K.O., A.N. and M.B.; Writing – Review & Editing, R.N., W.S., N.H.M., and O.G.; Visualization, D.U., M.B., A.N., and A.K.O.; Supervision, M.B., A.K.O., J.R., and W.S.; Project Administration, M.B. and A.K.O; Funding Acquisition, M.B., A.K.O., J.R. and W.S.

DECLARATION OF INTERESTS

Plansee SE and AVL List GmbH do have an interest in successful commercialization of SOFC-powered range extender systems. However, because this technology is not yet available on the market, there will be no direct benefits for the companies from publication of this study. Rather, we intend to inspire the scientific community to further pushing this technology forward and developing their SOFC systems accordingly.

Received: November 21, 2019
Revised: March 30, 2020
Accepted: April 24, 2020
Published: June 3, 2020

REFERENCES

1. McCollum, D.L., Wilson, C., Bevione, M., Carrara, S., Edelenbosch, O.Y., Emmerling, J., Guivarch, C., Karkatsoulis, P., Keppo, I., Krey, V., et al. (2018). Interaction of consumer preferences and climate policies in the global transition to low-carbon vehicles. Nat. Energy *3*, 664–673.
2. Rechberger, J., Reissig, M., and Lawlor, V. (2018). SOFC EV Range Extender Systems for Biofuels (Springer Fachmedien Wiesbaden).
3. Cano, Z.P., Banham, D., Ye, S., Hintennach, A., Lu, J., Fowler, M., and Chen, Z. (2018). Batteries and fuel cells for emerging electric vehicle markets. Nat. Energy *3*, 279–289.
4. Lawlor, V., Reissig, M., Makinson, J., and Rechberger, J. (2017). SOFC System for Battery Electric Vehicle Range Extension: Results of the First Half of the Mestrex Project. ECS Trans. *78*, 191–195.
5. MeStREx project uses ethanol fueled SOFCs in EV range-extenders. Fuel Cells Bull. *2016*, 2–3.
6. Brett, D.J.L., Atkinson, A., Brandon, N.P., and Skinner, S.J. (2008). Intermediate temperature solid oxide fuel cells. Chem. Soc. Rev. *37*, 1568–1578.
7. Eguchi, K., Kojo, H., Takeguchi, T., Kikuchi, R., and Sasaki, K. (2002). Fuel flexibility in power generation by solid oxide fuel cells. Solid State Ion. 152–153, 411–416.
8. Reissig, M., Mathé, J., Planitzer, S., Vötter, R., and Rechberger, J. (2015). Standalone Portable SOFC Power Generator for Autonomous Operation. ECS Trans. *68*, 143–150.
9. Tucker, M.C. (2010). Progress in metal-supported solid oxide fuel cells: A review. J. Power Sources *195*, 4570–4582.
10. Glenk, G., and Reichelstein, S. (2019). Economics of converting renewable power to hydrogen. Nat. Energy *4*, 216–222.
11. DOE (2012). Fuel Cell Technologies Office Multi-Year Research, Development, and Demonstration Plan (U.S. Department of Energy).
12. Botti, J.J. (2003). The revolution through evolution: delphi solid oxide fuel cell for APU and hydrogen reformation. ECS Proceedings: Volumes 2003–07, 16–30.
13. Botti, J.J., Grieve, M.J., and MacBain, J.A. (2005). Electric Vehicle Range Extension Using an SOFC APU. SAE Technical Paper 2005-01-1172, World Congress & Exhibition (SAE International).
14. Krishnan, V.V. (2017). Recent developments in metal-supported solid oxide fuel cells. Wiley Interdiscip. Rev. Energy Environ. *6*, E246.
15. Thaler, F., Udomsilp, D., Schafbauer, W., Bischof, C., Fukuyama, Y., Miura, Y., Kawabuchi, M., Taniguchi, S., Takemiya, S., Nenning, A., et al. (2019). Redox stability of metal-supported fuel cells with nickel/gadolinium-doped ceria anode. J. Power Sources *434*, 226751.
16. Boldrin, P., and Brandon, N.P. (2019). Progress and outlook for solid oxide fuel cells for transportation applications. Nat. Catal. *2*, 571–577.
17. Haydn, M., Ortner, K., Franco, T., Uhlenbruck, S., Menzler, N.H., Stöver, D., Bräuer, G., Venskutonis, A., Sigl, L.S., Buchkremer, H.-P., et al. (2014). Multi-layer thin-film electrolytes for metal supported solid oxide fuel cells. J. Power Sources *256*, 52–60.
18. Bischof, C., Nenning, A., Malleier, A., Martetschläger, L., Gladbach, A., Schafbauer, W., Opitz, A.K., and Bram, M. (2019). Microstructure optimization of nickel/gadolinium-doped ceria anodes as key to significantly increasing power density of metal-supported solid oxide fuel cells. Int. J. Hydrogen Energy *44*, 31475–31487.

19. Rojek-Wöckner, V.A., Opitz, A.K., Brandner, M., Mathé, J., and Bram, M. (2016). A novel Ni/ceria-based anode for metal-supported solid oxide fuel cells. J. Power Sources *328*, 65–74.

20. Udomsilp, D., Roehrens, D., Menzler, N.H., Bischof, C., de Haart, L.G.J., Opitz, A.K., Guillon, O., and Bram, M. (2017). High-Performance Metal-Supported Solid Oxide Fuel Cells by Advanced Cathode Processing. J. Electrochem. Soc. *164*, F1375–F1384.

21. Udomsilp, D., Thaler, F., Menzler, N.H., Bischof, C., de Haart, L.G.J., Opitz, A.K., Guillon, O., and Bram, M. (2019). Dual-Phase Cathodes for Metal-Supported Solid Oxide Fuel Cells: Processing, Performance, Durability. J. Electrochem. Soc. *166*, F506–F510.

22. Gerstl, M., Nenning, A., Iskandar, R., Rojek-Wöckner, V., Bram, M., Hutter, H., and Opitz, A.K. (2016). The Sulphur Poisoning Behaviour of Gadolinia Doped Ceria Model Systems in Reducing Atmospheres. Materials (Basel) *9*, 649.

23. Opitz, A.K., Gerstl, M., and Bram, M. (2019). Model System Supported Impedance Simulation of Composite Electrodes. Fuel Cells (Weinh.) *19*, 417–428.

24. Mogensen, M., Sammes, N.M., and Tompsett, G.A. (2000). Physical, chemical and electrochemical properties of pure and doped ceria. Solid State Ion. *129*, 63–94.

25. Tuller, H.L., and Nowick, A.S. (1977). Small polaron electron transport in reduced CeO2 single crystals. J. Phys. Chem. Solids *38*, 859–867.

26. Chueh, W.C., Hao, Y., Jung, W., and Haile, S.M. (2011). High electrochemical activity of the oxide phase in model ceria-Pt and ceria-Ni composite anodes. Nat. Mater. *11*, 155–161.

27. Adler, S.B., Lane, J.A., and Steele, B.C.H. (1996). Electrode Kinetics of Porous Mixed-Conducting Oxygen Electrodes. J. Electrochem. Soc. *143*, 3554–3564.

28. Nielsen, J., Jacobsen, T., and Wandel, M. (2011). Impedance of porous IT-SOFC LSCF:CGO composite cathodes. Electrochim. Acta *56*, 7963–7974.

29. Nenning, A., Gerstl, M., Bram, M., and Opitz, A.K. (2019). Mechanistic Insight into Porous Electrode Impedance: An Example of Ni+YSZ Cermet Anodes. ECS Trans. *91*, 479–490.

30. Nenning, A., Bischof, C., Fleig, J., Bram, M., and Opitz, A.K. (2020). The Relation of Microstructure, Materials Properties and Impedance of SOFC Electrodes: A Case Study of Ni/GDC Anodes. Energies *13*, 987.

31. Chueh, W.C., and Haile, S.M. (2009). Electrochemical studies of capacitance in cerium oxide thin films and its relationship to anionic and electronic defect densities. Phys. Chem. Chem. Phys. *11*, 8144–8148.

32. Jamnik, J., and Maier, J. (2001). Generalised equivalent circuits for mass and charge transport: chemical capacitance and its implications. Phys. Chem. Chem. Phys. *3*, 1668–1678.

33. Wang, S., Kobayashi, T., Dokiya, M., and Hashimoto, T. (2000). Electrical and Ionic Conductivity of Gd-Doped Ceria. J. Electrochem. Soc. *147*, 3606–3609.

34. Gerstl, M., Hutterer, A., Fleig, J., Bram, M., and Opitz, A.K. (2016). Model composite microelectrodes as a pathfinder for fully oxidic SOFC anodes. Solid State Ion. *298*, 1–8.

35. Iwai, H., Shikazono, N., Matsui, T., Teshima, H., Kishimoto, M., Kishida, R., Hayashi, D., Matsuzaki, K., Kanno, D., Saito, M., et al. (2010). Quantification of SOFC anode microstructure based on dual beam FIB-SEM technique. J. Power Sources *195*, 955–961.

36. Izzo, J.R., Joshi, A.S., Grew, K.N., Chiu, W.K.S., Tkachuk, A., Wang, S.H., and Yun, W. (2008). Nondestructive Reconstruction and Analysis of SOFC Anodes Using X-ray Computed Tomography at Sub-50 nm Resolution. J. Electrochem. Soc. *155*, B504–B508.

37. Kanno, D., Shikazono, N., Takagi, N., Matsuzaki, K., and Kasagi, N. (2011). Evaluation of SOFC anode polarization simulation using three-dimensional microstructures reconstructed by FIB tomography. Electrochim. Acta *56*, 4015–4021.

38. Mogensen, M.B., Hauch, A., Sun, X., Chen, M., Tao, Y., Ebbesen, S.D., Hansen, K.V., and Hendriksen, P.V. (2017). Relation Between Ni Particle Shape Change and Ni Migration in Ni–YSZ Electrodes – a Hypothesis. Fuel Cells (Weinh.) *17*, 434–441.

39. Tao, Y., Ebbesen, S.D., and Mogensen, M.B. (2016). Degradation of solid oxide cells during co-electrolysis of steam and carbon dioxide at high current densities. J. Power Sources *328*, 452–462.

40. Franco, T., Haydn, M., Mücke, R., Weber, A., Rüttinger, M., Büchler, O., Uhlenbruck, S., Menzler, N.H., Venskutonis, A., and Sigl, L.S. (2011). Development of Metal-Supported Solid Oxide Fuel Cells. ECS Trans. *35*, 343–349.

41. Franco, T., Haydn, M., Weber, A., Schafbauer, W., Blum, L., Packbier, U., Roehrens, D., Menzler, N.H., Rechberger, J., Venskutonis, A., et al. (2013). The Status of Metal-Supported SOFC Development and Industrialization at Plansee. ECS Trans. *57*, 471–480.

42. Han, F., Mücke, R., Van Gestel, T., Leonide, A., Menzler, N.H., Buchkremer, H.P., and Stöver, D. (2012). Novel high-performance solid oxide fuel cells with bulk ionic conductance dominated thin-film electrolytes. J. Power Sources *218*, 157–162.

43. Blum, L., de Haart, L.G.J., Malzbender, J., Menzler, N.H., Remmel, J., and Steinberger-Wilckens, R. (2013). Recent results in Jülich solid oxide fuel cell technology development. J. Power Sources *241*, 477–485.

44. Thaler, F., Nenning, A., Bischof, C., Udomsilp, D., de Haart, L.G.J., Opitz, A.K., and Bram, M. (2019). Optimized Cell Processing as the Key of High Electrochemical Performance of Metal-Supported Solid Oxide Fuel Cells. ECS Trans. *91*, 887–900.

45. Dogdibegovic, E., Wang, R., Lau, G.Y., and Tucker, M.C. (2019). High performance metal-supported solid oxide fuel cells with infiltrated electrodes. J. Power Sources, 91–98, 410-411.

46. Tucker, M.C. (2017). Development of High Power Density Metal-Supported Solid Oxide Fuel Cells. Energy Technol. (Weinheim) *5*, 2175–2181.

47. Nielsen, J., Persson, Å.H., Muhl, T.T., and Brodersen, K. (2018). Towards High Power Density Metal Supported Solid Oxide Fuel Cell for Mobile Applications. J. Electrochem. Soc. *165*, F90–F96.

48. Leah, R.T., Bone, A., Hammer, E., Selcuk, A., Rahman, M., Clare, A., Rees, L., Lawrence, N., Ballard, A., Domanski, T., et al. (2017). Development of High Efficiency Steel Cell Technology for Multiple Applications. ECS Trans. *78*, 2005–2014.

49. Ceres Power, Bosch in strategic collaboration, prepare for production. Fuel Cells Bull. 2018, 11.

50. Hickey, D., Alinger, M., Shapiro, A., Brown, K., Striker, T., Wang, H., Gaunt, S., Kinsey, D., and Hussaini, I. (2017). Stack Development at GE-Fuel Cells. ECS Trans. *78*, 107–116.

51. Wang, R., Dogdibegovic, E., Lau, G.Y., and Tucker, M.C. (2019). Metal-Supported Solid Oxide Electrolysis Cell with Significantly Enhanced Catalysis. Energy Technol. (Weinheim) *7*, 1801154.

52. Hoerlein, M.P., Riegraf, M., Costa, R., Schiller, G., and Friedrich, K.A. (2018). A parameter study of solid oxide electrolysis cell degradation: Microstructural changes of the fuel electrode. Electrochim. Acta *276*, 162–175.

53. Fang, Q., Frey, C.E., Menzler, N.H., and Blum, L. (2018). Electrochemical Performance and Preliminary Post-Mortem Analysis of a Solid Oxide Cell Stack with 20,000 h of Operation. J. Electrochem. Soc. *165*, F38–F45.

54. Frey, C.E., Fang, Q., Sebold, D., Blum, L., and Menzler, N.H. (2018). A Detailed Post Mortem Analysis of Solid Oxide Electrolyzer Cells after Long-Term Stack Operation. J. Electrochem. Soc. *165*, F357–F364.

55. Gross, S.M., Koppitz, T., Remmel, J., Bouche, J.-B., and Reisgen, U. (2006). Joining properties of a composite glass-ceramic sealant. Fuel Cells Bull. *2006*, 12–15.

56. Klemensø, T., Nielsen, J., Blennow, P., Persson, Å.H., Stegk, T., Christensen, B.H., and Sønderby, S. (2011). High performance metal-supported solid oxide fuel cells with Gd-doped ceria barrier layers. J. Power Sources *196*, 9459–9466.

Cell Reports Physical Science, Volume *1*

Supplemental Information

Metal-Supported Solid Oxide Fuel Cells with Exceptionally High Power Density for Range Extender Systems

David Udomsilp, Jürgen Rechberger, Raphael Neubauer, Cornelia Bischof, Florian Thaler, Wolfgang Schafbauer, Norbert H. Menzler, Lambertus G.J. de Haart, Andreas Nenning, Alexander K. Opitz, Olivier Guillon, and Martin Bram

Supplemental Experimental Procedures

General Information: The main manuscript outlines how fundamental research can contribute essentially to boost the electrochemical performance of metal-supported SOFCs manufactured on a pilot scale. To keep the balance between fundamental electrochemistry, processing, and full-cell performance, the main manuscript includes a concise summary of the fundamental electrochemical issues. Otherwise the electrochemistry part would go far beyond the scope of this paper. Therefore, the first part of this supplemental information provides details of the electrochemical experiments. In the same manner, a comprehensive benchmark of the state-of-the-art of metal-supported SOFCs in the main manuscript would divert attention from the main argumentation. Nevertheless, the interested reader can get information on the latest worldwide progress of metal-supported SOFCs in the second part of the supplementary information.

Impedance Characterization Results of Ni/GDC Fuel Electrodes: The effect of the functional layer thickness of the fuel electrodes on the polarization resistance can be seen from the impedance spectra depicted in **Figure S1**. The fit curves in this plot were obtained by CNLS-fitting using the equivalent circuit shown in **Figure 1b** of the main text. This circuit has an analytic impedance function:

$$Z = R_{YSZ} + \left(i(\omega Q_{int})^{p_{int}} + \frac{1}{R_{int}+Z_{TL}}\right)^{-1}.$$

Therein, R_{YSZ} is the electrolyte resistance, Q_{int} and p_{int} are the constant phase element parameters describing the interfacial capacitance (p_{int} was fixed to 0.8 to avoid over-parametrisation), R_{int} is the area-specific interfacial resistance and Z_{TL} is the transmission line modelling the fuel oxidation and ion conduction in the electrolyte by the equation

$$Z_{TL} = \sqrt{\frac{1}{\sigma_{eff} Y_{ec}}} \coth\left(l * \sqrt{R_{ion} Y_{ec}}\right),$$

where

$$Y_{ec} = \frac{1}{R_{react}} + (i\omega)^{pchem} C_{chem}.$$

The fit parameters are composite quantities, depending on microstructural and elementary material parameters of the Ni/GDC cermet structure. The geometry parameters result from analysis of SEM images (see Figure 2b in the main text) and 3D FIB-SEM reconstruction (data not shown here) – a GDC volume fraction ε_{GDC} of ca. 30 % and a tortuosity τ_{GDC} of about 3, were obtained.

For calculation of the effective free GDC surface area, two models were used: from SEM cross-sections, a mean GDC particle size of 270 nm is estimated, which have about 60 % of their surface atmosphere exposed and 40 % sintered on other GDC, or Ni grains. With 30 vol% GDC, such a microstructure has ~30 GDC particles per μm^3 and a free GDC surface of 4 $\mu m^2\ \mu m^{-3}$. The second surface area estimate relies on the BET surface of the GDC powder (8.1 $m^2\ g^{-1}$) before sintering. When we estimate that the atmosphere exposed surface area decreases by 65 % during sintering, this amounts to an average GDC surface area of 6 $\mu m^2\ \mu m^{-3}$. For the microscopic interpretation of our results, we used the average of both methods: $A_{spec} \approx 5\ \mu m^2\ \mu m^{-3}$.

With these microstructural parameters, the obtained fit parameters from impedance analysis can be used to calculate material specific values, which are summarized for all experimental temperatures in the Arrhenius plots in **Figure S2**:

(i) For the surface area specific reaction resistance $R_{surface}$ this is done by the relation

$$R_{surface} = R_{react}/A_{spec},$$

where R_{react} is the effective resistance of the fuel oxidation reaction in the cermet and A_{spec} is the specific surface area. By this method we obtain GDC surface resistances of ca. 4 Ω cm^2 at 650 °C and ca. 2 Ω cm^2 at 750 °C. Model studies on thin film GDC electrodes predict surface ASR values of 6 Ω cm^2 at 650°C [8] and 4 Ω cm^2 at 750°C [9]. The values obtained from the porous Ni/GDC electrodes (cf. Fig. 3) are thus in good agreement with literature expectations, especially when considering the still remaining uncertainty of determining the specific GDC surface area of the cermet and the degradation observed on thin film electrodes.

(ii) In addition to the reaction resistance, the GDC phase chemical capacitance is calculated by

$$C_{GDC} = \frac{C_{chem}}{\epsilon_{GDC}},$$

where ε_{GDC} is the volume fraction of GDC in the porous electrode. The GDC chemical capacitance can be compared to thermogravimetric isotherms, where oxygen non-stoichiometry is measured as function of $p(O_2)$ by tracking of the sample mass, e.g. by Wang et al. [10].

$$C_{chem} = \frac{8F^2V}{RTV_m} * \left| \frac{\boldsymbol{d\delta}}{\boldsymbol{d\ ln(pO_2)}} \right|$$

(iii) The GDC phase ion conductivity σ_{ion} and effective ion conductivity σ_{eff} are coupled by the relation.

$$\sigma_{ion} = \sigma_{eff} * \frac{\tau_{GDC}}{\epsilon_{GDC}}$$

The conductivity of dense GDC polycrystals is available in literature, e.g. [11].

(iv) The electrochemically active thickness λ, determining the extension of the reaction zone from the electrolyte is obtained by 12

λ=√(R_react*σ_eff).

All of the above mentioned relations are used to obtain the diagrams of **Figure S2**, showing Arrhenius plots of impedance fitting results of two electrodes with equal processing and testing conditions (45 mbar H_2 + 25 mbar H_2O) and two different thicknesses, achieved through different screen printing meshes. Four samples for each thickness were measured, and mean values + error bars are depicted.

Note S1

Benchmarking of MSC concepts: An overview of the electrochemical performance of MSCs achieved on single-cell level over the past 15 years is given in **Table S1** for summarizing the state-of-the-art of the main MSC concepts. For better comparison, all current densities are given – if available – at a cell voltage of 0.7 V and at an operating temperature of 700 °C. Nevertheless, it must be considered that objective benchmarking of these MSC concepts is limited by differences in test rigs, testing conditions, cell sizes, and gas compositions used by the different research groups. In general, clear improvement of the electrochemical performance of MSCs was demonstrated by several groups driven by the high requirements automotive companies place on MSCs for the application in range extenders.

Various approaches resulted in enhanced cell performance. At 0.7 V and 700 °C, Gao et al. [13] achieved a current density of 1.5 A cm^{-2} with an MSC button cell made by low-pressure plasma spraying. Nielsen et al. [14] at DTU (Denmark) reported a current density of 1.44 A cm^{-2} and Tucker [15-17] at LBNL (USA) obtained current densities of 1.5-2.2 A cm^{-2}. The MSC concepts of Nielsen and Tucker are based on lamination and co-firing of electrolyte, porous ceramic backbones, and metal tapes, which are subsequently infiltrated with precursor solutions for fabricating nanosized active particles in at least one of the electrodes. In the MSC concept of Ceres Power, the maximum operating temperature is limited to 600 °C due to the application of a gadolinium doped ceria (GDC) electrolyte, as electronic conductivity induced by reduction of Ce^{4+} to Ce^{3+} in the GDC electrolyte leads to internal short-circuiting and loss of performance [18,19]. The electrodes and the electrolyte are applied on a perforated Fe/Cr steel substrate and sintered at T < 1100 °C in air [20-23]. A performance of 0.3-0.4 A cm^{-2} is reported at a cell voltage of 0.75 V and 600 °C [22]. A common feature of these cell concepts is the use of a cermet made from Ni and doped ceria confirming its high electrochemical activity as anode material. The metal-supported design enables the utilization of doped ceria in the anode in combination with a stabilized zirconia electrolyte without facing the problem of secondary phases formed during high-temperature co-sintering of doped ceria and zirconia-based electrolytes as is the case in the fabrication of ASCs [24].

The cell design in the presented work – apart from the Ceres Power setup – is the only one which is not based on infiltration techniques in order to achieve highly active electrode microstructures. This is the basis for enhanced long-term stability in contrast to electrode structures prepared by infiltration of nanoparticles which tend to coarsen during operation, thus degrading cell performance. At the same time, the present design enables flexibility with regard to the optimum operating temperature for different applications. Furthermore, the processing steps are suitable for an automated production, which is required for reliable quality of the cells, and they allow for further microstructural optimization of the electrodes.

The Gen 3 cell performance of 2.8 A cm^{-2} (0.7 V, 650 °C) and 0.89 A cm^{-2} (0.9 V, 650 °C) on 16 cm^2 cells is an excellent result in comparison to other metal-supported SOFCs reported in the literature. The high current density even at 650 °C provides the possibility of designing stacks with high power density close to the performance targets identified in the analysis of this work (c.f. Table 1 in the main text). Hence, the presented metal-supported SOFCs are a major step towards industrially viable range extender systems. Design and fabrication of stacks are the next steps needed to exploit the high performance of the Gen 3 cell in range extender applications.

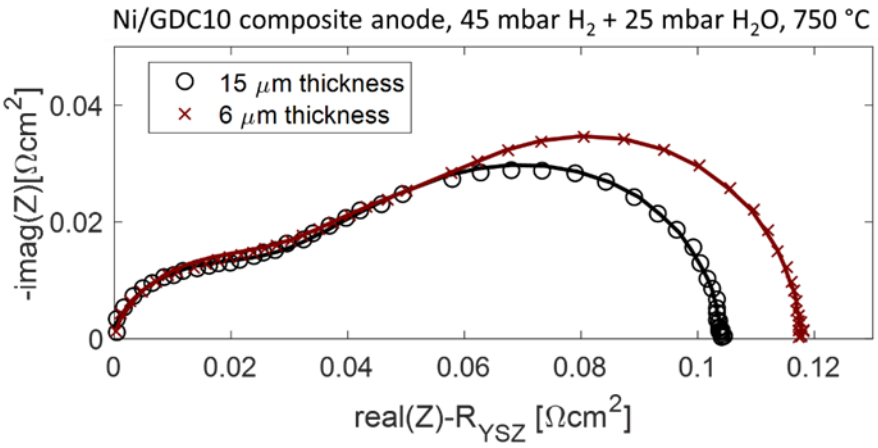

Figure S1: Impedance spectrum of Ni/GDC cermet anodes with two different fuctional layer thicknesses (symbols) together with the respective fit curves (lines) using the equivalent circuit in **Figure 1b**.

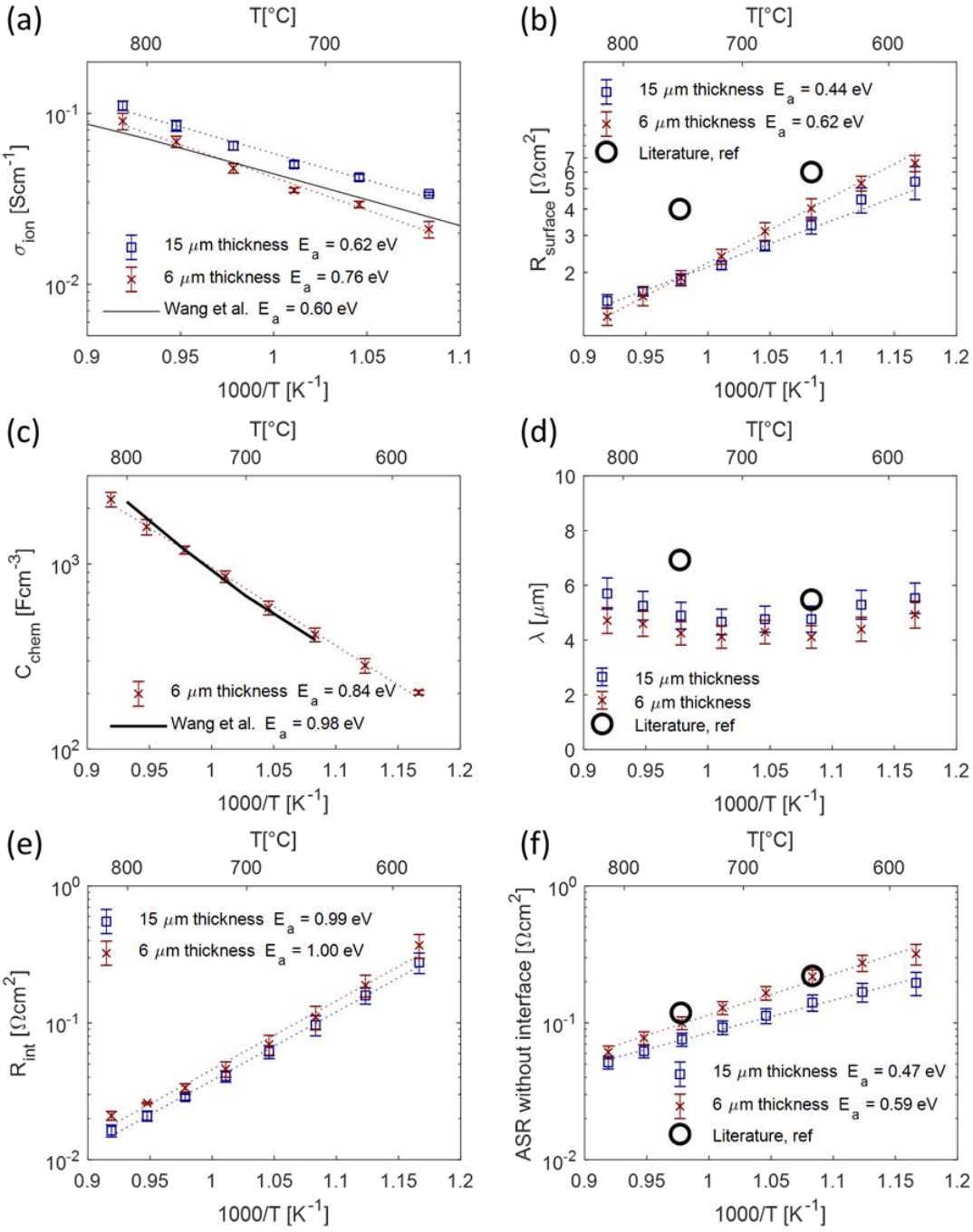

Figure S2: Materials parameters, gained from CLNS fitting (blue squares, red crosses), compared to literature values: **(a)** GDC phase ionic conductivity; reference: conductivity of polycrystal[11]. **(b)** Surface area specific resistance of the hydrogen oxidation reaction, **(c)** GDC phase chemical capacitance, compared to thermogravimetric measurements **(d)** electrochemically active thickness, **(e)** area-related resistance of the YSZ-GDC interface, **(f)** ASR of the electrochemical electrode processes, after subtraction of the interfacial resistance.

Table S1: Electrochemical performance of MSCs from selected research groups. All tests were done using H_2/H_2O as fuel and air as oxidant. [GDC – $(Ce,Gd)O_{2-\delta}$; LSCF – $(La,Sr)(Co,Fe)O_{3-\delta}$; SDC – $(Ce,Sm)O_{2-\delta}$; ScYSZ – $(Sc,Y,Zr)O_{2-\delta}$; ScSZ – $(Sc,Ce,Zr)O_{2-\delta}$; LSM – $(La,Sr)MnO_{3-\delta}$; BSCF – $(Ba,Sr)(Co,Fe)O_{3-\delta}$; *) extrapolated]

Authors	Year	Anode	Electrolyte	Cathode	Active area [cm²]	Test parameters	$j_{0,7V}$ [A cm^{-2}]	$P_{0,7V}$ [W cm^{-2}]
Brandon et al. [25]	2004	Ni/GDC	GDC	LSCF/GDC	16	550 °C	0.25	0.18
Brandner et al. [26]	2008	Ni/YSZ	9.5YSZ	LSCF	16	803 °C	0.60	0.42
Blennow et al. [27]	2011	Ni/GDC infiltrated	ScYSZ	LSC	0.5	700 °C	0.9	0.63
Klemensø et al. [28]	2011	Ni/GDC infiltrated	ScYSZ	LSC	0.5	650 °C	1.5	1.05
Kesler et al. [29]	2013	Cu/Co/Ni/SDC	YSZ	LSCF-SDC	Not stated	700 °C	0.50	0.35
Rojek-Woeckner et al. [2]	2016	Ni/GDC	YSZ	LSCF	16	700 °C	0.75	0.53
Gao et al. [13]	2017	Ni/GDC	GDC	LSM/BSCF	0.5	700 °C	1.5	1.05
Haydn et al. [3]	2017	Ni/GDC	YSZ	LSCF	0.64	700 °C	1.6	1.1
Leah et al. [22]	2017	Ni/GDC	GDC/YSZ	LSCF	Not stated	600 °C	0.53 (0.75 V)	0.40 (0.75 V)
Tucker [15]	2017	SDC/Ni/YSZ infiltrated	YSZ	LSM/YSZ infiltrated	1…4	700 °C	1.5	1.05
Nielsen et al. [14]	2018	Ni/GDC infiltrated	ScSZ	LSC	16	700 °C	1.44	1.01
Dogdibegovic [16]	2019	SDC/Ni infiltrated	ScSZ	Pr_6O_{11} infiltrated	1	700 °C	2.2	1.5
This work	2020	Ni/GDC	YSZ	LSC	16	700 °C	3.6 *)	2.5 *)
This work	2020	Ni/GDC	YSZ	LSC	16	700 °C	1.34 (0.9 V)	1.21 (0.9 V)

Supplemental References

1. Haydn M, Ortner K, Franco T, Uhlenbruck S, Menzler NH, Stöver D, et al. Multi-layer thin-film electrolytes for metal supported solid oxide fuel cells. Journal of Power Sources. 2014;256:52-60.
2. Rojek-Wöckner VA, Opitz AK, Brandner M, Mathé J, Bram M. A novel Ni/ceria-based anode for metal-supported solid oxide fuel cells. Journal of Power Sources. 2016;328:65-74.
3. Haydn M, Bischof C, Udomsilp D, Opitz AK, Bimashofer G, Schafbauer W, et al. Metal Supported SOFCs: Electrochemical Performance under Various Testing Conditions. ECS Transactions. 2017;78(1):1993-2003.
4. Opitz AK, Gerstl M, Bram M. Model System Supported Impedance Simulation of Composite Electrodes. Fuel Cells. 2019;19(4):417-28.
5. Udomsilp D, Roehrens D, Menzler NH, Bischof C, de Haart LGJ, Opitz AK, et al. High-Performance Metal-Supported Solid Oxide Fuel Cells by Advanced Cathode Processing. Journal of The Electrochemical Society. 2017;164(13):F1375-F84.
6. Udomsilp D. Charakterisierung und Optimierung der Grenzfläche Elektrolyt/Kathode in metallgestützten Festelektrolyt-Brennstoffzellen. Jülich: Forschungszentrum Jülich GmbH Zentralbibliothek, Verlag; 2018.
7. Thaler F, Nenning A, Bischof C, Udomsilp D, de Haart LGJ, Opitz AK, et al. Optimized Cell Processing as the Key of High Electrochemical Performance of Metal-Supported Solid Oxide Fuel Cells. ECS Transactions. 2019;91(1):887-900.
8. Chueh WC, Hao Y, Jung W, Haile SM. High electrochemical activity of the oxide phase in model ceria–Pt and ceria–Ni composite anodes. Nature Materials. 2011;11:155.
9. Gerstl M, Hutterer A, Fleig J, Bram M, Opitz AK. Model composite microelectrodes as a pathfinder for fully oxidic SOFC anodes. Solid State Ionics. 2016;298:1-8.
10. Wang S, Inaba H, Tagawa H, Dokiya M, Hashimoto T. Nonstoichiometry of Ce0.9Gd0.1O1.95−x. Solid State Ionics. 1998;107(1):73-9.
11. Wang S, Kobayashi T, Dokiya M, Hashimoto T. Electrical and Ionic Conductivity of Gd-Doped Ceria. Journal of The Electrochemical Society. 2000;147(10):3606-9.
12. Nenning A, Gerstl M, Bram M, Opitz AK. Mechanistic Insight into Porous Electrode Impedance: An Example of Ni+YSZ Cermet Anodes. ECS Transactions. 2019;91(1):479-90.
13. Gao J-T, Wang Y-P, Li C-X, Zhang S-L, Yang G-J, Li C-J. Study on the Fabrication and Performance of Very Low Pressure Plasma Sprayed Porous Metal Supported Solid Oxide Fuel Cell. ECS Transactions. 2017;78(1):2059-67.
14. Nielsen J, Persson ÅH, Muhl TT, Brodersen K. Towards High Power Density Metal Supported Solid Oxide Fuel Cell for Mobile Applications. Journal of The Electrochemical Society. 2018;165(2):F90-F6.
15. Tucker MC. Development of High Power Density Metal-Supported Solid Oxide Fuel Cells. Energy Technology. 2017;5(12):2175-81.
16. Dogdibegovic E, Wang R, Lau GY, Tucker MC. High performance metal-supported solid oxide fuel cells with infiltrated electrodes. Journal of Power Sources. 2019;410-411:91-8.
17. Tucker MC. Metal-Supported Solid Oxide Fuel Cell with High Power Density. ECS Transactions. 2017;78(1):2015-20.
18. Steele BCH, Heinzel A. Materials for fuel-cell technologies. Nature. 2001;414:345.
19. Wachsman ED, Lee KT. Lowering the Temperature of Solid Oxide Fuel Cells. Science. 2011;334(6058):935-9.
20. Bance P, Brandon NP, Girvan B, Holbeche P, O'Dea S, Steele BCH. Spinning-out a fuel cell company from a UK University—2 years of progress at Ceres Power. Journal of Power Sources. 2004;131(1–2):86-90.
21. Leah R, Lankin M, Pierce R, Bone A. Process for Forming a Metal Supported Solid Oxide Fuel Cell. Google Patents; 2015.
22. Leah RT, Bone A, Hammer E, Selcuk A, Rahman M, Clare A, et al. Development of High Efficiency Steel Cell Technology for Multiple Applications. ECS Transactions. 2017;78(1):2005-14.
23. Leah RT, Bone A, Lankin M, Selcuk A, Rahman M, Clare A, et al. Ceres Power Steel Cell Technology: Rapid Progress Towards a Truly Commercially Viable SOFC. ECS Transactions. 2015;68(1):95-107.
24. Lenser C, Jeong H, Sohn YJ, Russner N, Guillon O, Menzler NH. Interaction of a ceria-based anode functional layer with a stabilized zirconia electrolyte: Considerations from a materials perspective. Journal of the American Ceramic Society. 2018;101(2):739-48.

25. Brandon NP, Corcoran D, Cummins D, Duckett A, El-Khoury K, Haigh D, et al. Development of metal supported solid oxide fuel cells for operation at 500–600 °C. J of Materi Eng and Perform. 2004;13(3):253-6.
26. Brandner M, Bram M, Froitzheim J, Buchkremer HP, Stöver D. Electrically Conductive Diffusion barrier layers for Metal-Supported SOFC. Solid State Ionics. 2008;179(27):1501-4.
27. Blennow P, Hjelm J, Klemensø T, Persson ÅH, Ramousse S, Mogensen M. Planar Metal-Supported SOFC with Novel Cermet Anode. Fuel Cells. 2011;11(5):661-8.
28. Klemensø T, Nielsen J, Blennow P, Persson ÅH, Stegk T, Christensen BH, et al. High performance metal-supported solid oxide fuel cells with Gd-doped ceria barrier layers. Journal of Power Sources. 2011;196(22):9459-66.
29. Kesler O, Cuglietta M, Harris J, Kuhn J, Marr M, Metcalfe C. Progress in Metal-Supported SOFCs Using Hydrogen and Methane Fuels. ECS Transactions. 2013;57(1):491-501.